Pronounced Cluster-Size Effects: Gas-Phase Reactivity of Bare Vanadium Cluster Cations V_n^+ ($n = 1-7$) Toward Methanol

Sandra Feyel,[†] Detlef Schröder,*[,‡] and Helmut Schwarz*[,†]

Institut für Chemie der Technischen Universität Berlin, Strasse des 17. Juni 135, D-10623 Berlin, Germany, and Institute of Organic Chemistry and Biochemistry, Academy of Sciences of the Czech Republic, Flemingovo nám. 2, 16610 Prague 6, Czech Republic

Received: February 20, 2009; Revised Manuscript Received: March 23, 2009

Mass spectrometric experiments are used to examine the size-dependent interactions of bare vanadium cluster cations V_n^+ ($n = 1-7$) with methanol. The reactivity patterns exhibit enormous size effects throughout the range of clusters investigated. For example, dehydrogenation of methanol to produce V_nOC^+ is only brought about by clusters with $n \geq 3$. Atomic vanadium cation V^+ also is reactive, but instead of dehydrogenation of the alcohol, expulsions of either methane or a methyl radical take place. In marked contrast, the reaction efficiency of the dinuclear cluster V_2^+ is extremely low. For the cluster cations V_n^+ ($n = 3-7$), complete and efficient dehydrogenation of methanol to produce V_nOC^+ and two hydrogen molecules prevails. DFT calculations shed light on the mechanism of the dehydrogenation of methanol by the smallest reactive cluster cation V_3^+ and propose the occurrence of chemisorption concomitant with C−O bond cleavage rather than adsorption of an intact carbon monoxide molecule by the cluster.

Introduction

Understanding the mechanistic details of the dehydrogenation of hydrocarbons and of small alcohols on metal surfaces constitutes a major challenge in contemporary catalysis. Although the properties of both clean and oxygen-modified surfaces have been studied from different perspectives in recent years, with currently available surface science techniques, the identification and characterization of the active sites and their catalytic interactions with a molecule are all but completely understood.[1,2] For example, the chemical nature of nanoparticle/product interactions is of essential interest as the adsorbates on the metal surface may strongly affect catalytic properties.[3] Controlled by the strength of this interaction, that is, dissociative versus nondissociative binding, the adsorbed product also can be detached from the surface in the course of the reaction, thus regenerating the catalyst. So far, there is consensus that dissociative binding is usually favored for early rather than late transition metals.[4]

With the catalyst particles getting smaller, free clusters in the gas phase provide an excellent testing ground for probing basic adsorption and/or chemisorption phenomena.[5,6] The reactions of gaseous transition-metal clusters with small molecules have formed the subject of numerous studies to elucidate the dependence of reactivity on cluster size.[7] It turned out that smaller clusters are unique in exhibiting enormous size effects in terms of, for instance, reactivity.[8] Vanadium as well as its oxides are particularly interesting catalysts with frequent uses in the chemical industry.[9] In the reactions of neutral V_m clusters ($m = 1-30$) with ethylene and acetylene, the dehydrogenated products V_mC_2 were generated concomitantly with elimination of molecular hydrogen, with a sudden reactivity increase for clusters with $m \geq 3$.[10,11] Here, we report an investigation of the reactivity of cationic, bare vanadium clusters V_n^+ ($n = 1-7$) toward methanol, with particular attention to the size-dependent dehydrogenation activity of V_n^+.[12,13]

Experimental and Computational Methods

Ion/molecule reactions (IMRs) are investigated using a Spectrospin CMS 47X FT-ICR mass spectrometer equipped with an external ion source, as described elsewhere.[14] In brief, bare vanadium cations V_n^+ ($n = 1-7$) are generated by laser ablation of a vanadium target using a Nd:YAG laser operating at 1064 nm. The hot vanadium plasma is cooled by the expanding helium gas (~20 bar, pulse time ~110 μs) and travels through a metal tube in which clustering takes place. A series of potentials and ion lenses are used to transfer the ions to the ICR cell, which is positioned in the bore of a 7.05 T superconducting magnet. In this manner, distributions of V_n^+ clusters up to $n = 10$ can be generated. All mass selections are performed using the FERETS protocol,[15] a computer-controlled routine that combines frequency sweeps and single frequency shots to optimize ion isolation. The metal cations, V_n^+ ($n = 1-7$),[16] are first mass-selected, then thermalized, and finally exposed to reactions with methanol in order to monitor their reactivities at a constant reaction pressure of methanol of about 5×10^{-9} mbar. After calibration of the measured pressures and acknowledgment of the ion gauge sensitivities,[17] branching ratios (BR) and rate constants are derived from the analysis of the reaction kinetics and are reported within an error of ±30%.[18] Reaction efficiencies $\varphi = k/k_{cap}$ were calculated according to capture theory.[19] Within experimental error, all primary reactions described below show strict pseudo-first-order behavior, thus supporting the assumed equilibration of the ions to 298 K. All unlabeled and labeled reagents were used as purchased and introduced into the FT-ICR cell by conventional vacuum techniques.

As a complement to the experimental work, the V_3^+/methanol system is studied by computational methods using density

* To whom correspondence should be addressed. Fax: 420 220 183 462. E-mail: Detlef.Schroeder@uochb.cas.cz (D.S.); Fax: 49 30 314 21102. E-mail: Helmut.Schwarz@mail.chem.tu-berlin.de (H.S.).
[†] Institut für Chemie der Technischen Universität Berlin.
[‡] Academy of Sciences of the Czech Republic.

10.1021/jp901565r CCC: $40.75
Published on Web 04/16/2009

SCHEME 1: Primary Reactions of V_n^+ with Methanol[a]

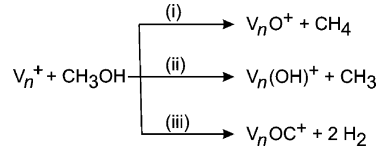

[a] For further details, see Table 1. For a classification of the observed reaction in terms of product channels (i)−(iii), see the text.

functional theory (DFT) as this cluster is still small enough to allow reasonably reliable quantum chemical calculations. Potential energy surfaces were explored using the Gaussian 03W suite of programs.[20] DFT calculations were carried out with the nonempirical PW91 exchange component of Perdew and Wang[21] in conjunction with the VWN[22] local exchange-correlation functional; the choice of this particular functional was inspired by an extensive computational study of the neutral and cationic V_3 cluster by Calaminici et al.[23] A modified TZVP basis set was employed;[24] this is the original TZVP set with an additional f-function for the vanadium atom. The exponents and contraction coefficients of the GGA-optimized TZVP basis set for vanadium, oxygen, carbon, and hydrogen atoms are compiled in the Supporting Information. All stationary points reported below were characterized by frequency analysis in order to discriminate between minima, transition structures, and higher-order saddle points. Further, intrinsic reaction coordinate (IRC) calculations[25] were performed to link transition structures with the intermediates shown in Figure 4. Unscaled frequencies were used, and the energies were corrected for zero-point vibrational energy contributions.

Results and Discussion

Experimental Findings. In the present work, laser ablation is used to generate bare vanadium cluster cations in the gas phase, followed by reacting the mass-selected cations with methanol and monitoring the time dependencies of the reactant and product ion intensities using a FT-ICR mass spectrometer. The focus of this article lies on the dehydrogenation activity of the V_n^+ ($n = 1-7$) cluster cations.

In the ion/molecule reactions (IMRs) of V_n^+ cations with methanol, three major primary processes are observed (Scheme 1, Table 1), (i) deoxygenation of methanol concomitant with liberation of methane to generate V_nO^+ ions ($\Delta m = +16$), (ii) abstraction of a hydroxy group from methanol concomitant with the release of a $CH_3^\bullet$ radical to produce V_nOH^+ ($\Delta m = +17$), and (iii) complete dehydrogenation of methanol to generate V_nOC^+ ($\Delta m = +28$); the latter process, on energetic grounds, is associated with the formation of two hydrogen molecules as the neutral products. We note that if not stated otherwise, throughout this article, the notation V_nOC^+ stands for either $V_n(CO)^+$ with an intact carbon monoxide molecule attached to the cluster or $V_n(O)(C)^+$ with two separate atoms incorporated in the cluster. Oxidation of methanol to produce formaldehyde is not observed. CH_2O is neither released as a neutral molecule concomitant with generation of $V_n(H_2)^+$ nor bound to the cluster to form $V_n(OCH_2)^+$ combined with the elimination of H_2. Likewise, none of the corresponding adduct complexes, $V_n(CH_3OH)^+$, have been observed under the conditions chosen.

The branching ratios (BRs) of the reaction channels are summarized in Table 1. The reaction of atomic vanadium cation V^+ with methanol ($k_{abs} = 2.5 \times 10^{-10}$ cm^3 molecule^{-1} s^{-1}) results in the formation of the vanadium oxide cation VO^+ concomitant with the liberation of methane. This process is strongly exothermic, $\Delta_r H = -204$ kJ mol^{-1}.[26a] Further, loss of a methyl radical by OH abstraction occurs as well to produce VOH^+ ($\Delta_r H = -46$ kJ mol^{-1}).[26a] For the mononuclear system, also, a signal due to the vanadium methoxide cation, $V(OCH_3)^+$ is observed; this product is also formed in a consecutive condensation reaction of the primary product VOH^+ with a second methanol molecule.[26] Elimination of two hydrogen molecules from methanol concomitant with formation of VOC^+ does not take place for the mononuclear species.

TABLE 1: Absolute Biomolecular Rate Constants (k_{abs}), Reaction Efficiencies (φ), Mass Differences (Δm given in amu), and Branching Ratios (BR with $\Sigma BR_i = 100$) in the IMRs of V_n^+ Clusters with Methanol ($p(CH_3OH) = 5 \times 10^{-9}$ mbar)

			Δm		
V_n^+	$k_{abs} \times 10^{-10}$ cm^3 molecule^{-1} s^{-1}[a]	φ	+16	+17	+28
V^+[b]	2.5	0.10	30	60	
V_2^+[c]	0.5	0.02	35	45	5
V_3^+	3.0	0.16	15	20	65
V_4^+	4.5	0.25	5	15	80
V_5^+	8.4	0.45	15	10	75
V_6^+[d]			s	s	m
V_7^+[d]					m

[a] The error bars are estimated to ±30%. [b] IMR of V^+ resulted also in formation of $V(OCH_3)^+$ (BR = 10%). [c] V_2^+ also undergoes fragmentation upon oxygen uptake to form VO^+ (BR = 15%). [d] The quality of the spectra obtained for the V_6^+/methanol and V_7^+/methanol systems is insufficient for a quantitative evaluation. Phenomenological notation of signal abundances: s = small; m = major.

The IMR of the dinuclear vanadium cation V_2^+ with methanol results in the formation of the corresponding vanadium oxide and hydroxide cations, V_2O^+ and V_2OH^+, respectively. The overall rate constant is rather low, however ($k_{abs} = 0.5 \times 10^{-10}$ cm^3 molecule^{-1} s^{-1}). Furthermore, a reaction pathway leading to complete dehydrogenation of methanol to produce V_2OC^+ occurs with even much lower abundance.

In perfect analogy the IMR of V_3^+ with methanol results in the cations V_3O^+ and V_3OH^+. In addition, however, double dehydrogenation is observed to afford V_3OC^+ from V_3^+ with methanol, and this reactions thus involves the smallest bare vanadium cluster cation being capable of entirely dehydrogenating methanol efficiently ($k_{abs} = 3.0 \times 10^{-10}$ cm^3 molecule^{-1} s^{-1}; Table 1). The larger vanadium cations V_n^+ with $n = 4-7$ all follow the reaction scenario of V_3^+ and produce V_nO^+, V_nOH^+, and V_nOC^+ ($n = 4-7$), respectively.

Not surprisingly, upon increasing the cluster size n, the absolute rate constants k_{abs} of the reactions increase as well (Table 1). This result is consistent with larger lifetimes of the encounter complexes for the larger cluster ions, because the energy gain from association with the substrate can be redistributed more efficiently within the cluster. As redissociation into the reactants is less likely, the probability to form products becomes higher for larger clusters than for smaller ones.[27]

Figure 1 shows the efficiencies of the reaction channels (i)−(iii) as a function of cluster size for $n = 1-5$. Upon increasing the cluster size, the signals of V_nO^+ and V_nOH^+ decrease or do not vary that much, whereas those of V_nOC^+ exhibit a sharp threshold at $n = 2 \rightarrow 3$ and then increase continuously. This experimental finding agrees well with previous observations of Nonose et al., who also reported a sudden increase in the reactivity with cluster size of bare, neutral vanadium clusters ($n = 3-5$) with respect to the dehydrogenations of ethene and ethyne.[10]

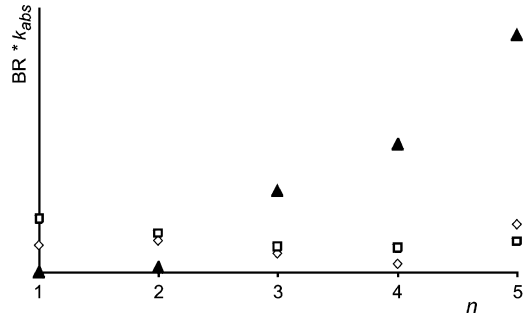

Figure 1. Experimental rate constant k_{abs} multiplied with the branching ratio (BR) versus the cluster size n ($n = 1-5$). Black triangles: V_nOC^+; open squares: V_nOH^+; open diamonds: V_nO^+.

Before we further focus on the complete dehydrogenation of methanol (pathway (iii) in Scheme 1), let us briefly return to the vanadium oxide and hydroxide products. When the V_n^+ cluster cations ($n = 1-4$) are reacted with water ($p(H_2O) = 5 \times 10^{-9}$ mbar), V_nO^+ is observed as the exclusive product, whereas no V_nOH^+ species are detected. A similar reactivity had been reported earlier by Koyanagi et al.[28] in the reaction of bare V^+ with water. The formation of the hydroxide clusters in the reactions with methanol and in its absence in the V_n^+/H_2O systems can thus be associated with the weaker CH_3-OH bond of methanol (385 kJ mol^{-1}) as compared to the much stronger H−OH bond of water (497 kJ mol^{-1}).[29]

Furthermore, the vanadium oxide products, V_nO^+, may not only be formed due to interaction with gaseous methanol because labeling experiments of V_n^+ ($n = 1, 3, 4$) with $CH_3{}^{18}OH$ reveal that, in addition to the generation of $V_n{}^{18}O^+$, also the lighter congeners $V_n{}^{16}O^+$ are produced. Note, that the ratio of $V_n{}^{18}O^+/V_n{}^{16}O^+$ is only around 0.3 for the tri- and tetranuclear species. Obviously, as the lighter oxides $V_n{}^{16}O^+$ cannot originate from heavy methanol, any impurities (most likely O_2) remaining in the cell serve as precursors.[14a,28,30] Accordingly, the branching ratios obtained for V_nO^+ in the IMRs of V_n^+ with light methanol do not exclusively reflect the reactions with the alcohol but also contain contributions from background impurities. As these exhibit typical day-to-day variations, the BRs given for V_nO^+ are not corrected any further.

As mentioned in the Introduction, the focus of this study is to provide an understanding of the complete dehydrogenation of methanol to bring about the formation of V_nOC^+. In this respect, basically two different structural features are conceivable for the product ion; either a genuine metal carbonyl cluster, that is, $V_n(CO)^+$, is produced with a carbon monoxide unit being bound to the cluster cation, or chemisorption occurs to generate a $V_n(O)(C)^+$ species with the O- and C-atoms being separately bonded to the vanadium atoms of the cationic cluster. With regard to implications for catalysis, the former product offers the advantage of a more or less effortless recovery of V_n^+, whereas catalyst recovery might be significantly more difficult for the latter structure.

In order to enable a structural characterization of both potential products, the V_3OC^+ cation evolving from the reaction of V_3^+ with methanol was mass-selected and exposed to a pulse of labeled carbon monoxide, ^{13}CO, aiming at an expected ligand exchange[31] of the intact light CO molecule by ^{13}CO. However, the mass-selected primary product cation, V_3OC^+, does not show any significant amount of $^{12}C/^{13}C$ exchange; rather, it undergoes secondary reactions with residual methanol to repeat the given reaction pattern, producing secondary products such as $V_3(O)OC^+$, $V_3(OH)OC^+$, and $V_3O_2C_2^+$. This experiment suggests a dissociative binding of the carbon monoxide, that is, chemisorption via formation of the $V_n(O)(C)^+$ cluster cation in the course of methanol dehydrogenation. However, the fact that the reaction channel for $^{12}C/^{13}C$ exchange is not observed in our experiment is not definitive proof for its nonexistence. We further note that collision-induced dissociation of V_3OC^+ using an argon pulse with the intention to monitor loss of a neutral CO molecule from V_3OC^+ failed due to too low fragment ion abundance.

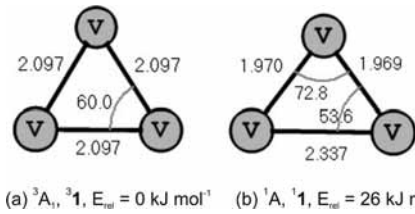

Figure 2. Optimized structures of V_3^+ for (a) $^3A_1$ (^{3}**1**) and (b) ^1A (^{1}**1**). Bond lengths are given in Ångströms and bond angles in degrees.

Noteworthy in this context is a recent study of de Groot and co-workers,[32] who examined the size-dependent interaction of carbon monoxide with hydrogen-covered vanadium cluster cations containing between 5 and 20 atoms. They reported the prevention of dissociative chemisorption when the potential binding sites for atomic C- and O-atoms are blocked by H-atoms.[32] Accordingly, completely H-covered vanadium cluster cations stabilize the coadsorbed CO complex against the thermochemically favorable dissociative chemisorption, whereas vacant sites on the vanadium cluster accommodate the C- and O-atoms, thus enabling dissociation of an intact CO ligand. In the present context, the question emerges whether this also holds true for the smaller bare vanadium cluster cations, that is, can the bare V_n^+ investigated in this work also permit the dissociation of the "fleeting" CO molecule formed from methanol.

Computational Findings. To elucidate the relative energetics of the two isomeric ionic products, that is, to probe whether $V_n(CO)^+$ or $V_n(O)(C)^+$ is formed in the course of the reaction, and further to shed light on the overall reaction profile, we applied density functional theory (DFT). As V_3^+ is the smallest bare vanadium cluster cation to afford efficiently the complete dehydrogenation of methanol, the potential energy surface of the V_3^+/CH_3OH system was chosen for a closer inspection. Nevertheless, it is not the aim of this article to map out the complete mechanistic reaction scenario. Rather, the suggested mechanism may turn out to be just one of several plausible pathways, and we explicitly do not exclude other routes. Moreover, we would like to point out explicitly that a more detailed investigation using wave-function-based methods, for example, coupled cluster approaches, could be used to evaluate the reliability of the predictions derived from DFT calculations. Previous work of several theoretical groups demonstrated that the differences between DFT and CCSD(T) energies can even exceed 50 kJ mol^{-1};[31a,33] an extension of the present work to the CCSD(T) level of theory is far beyond our scope, however.

Figure 2 summarizes the optimized structures of V_3^+ for the triplet and singlet states.[23] The former one is energetically more favored for cationic V_3^+, yielding an equilateral triangular $^3A_1$ ground state (^{3}**1**). Singlet V_3^+ (^{1}**1**) is predicted as an almost isosceles triangle (Figure 2b) lying 26 kJ mol^{-1} above the triplet state. Accordingly, all energies discussed further below are given relative to the triplet surface of the entrance channel of separated V_3^+ ($^3A_1$) and methanol. Likewise, the relative energies for the products are calculated for V_3OC^+ and two separate H_2 molecules.

Product Ion. At first, let us address the net energetics of the two different reaction scenarios, that is, associative versus

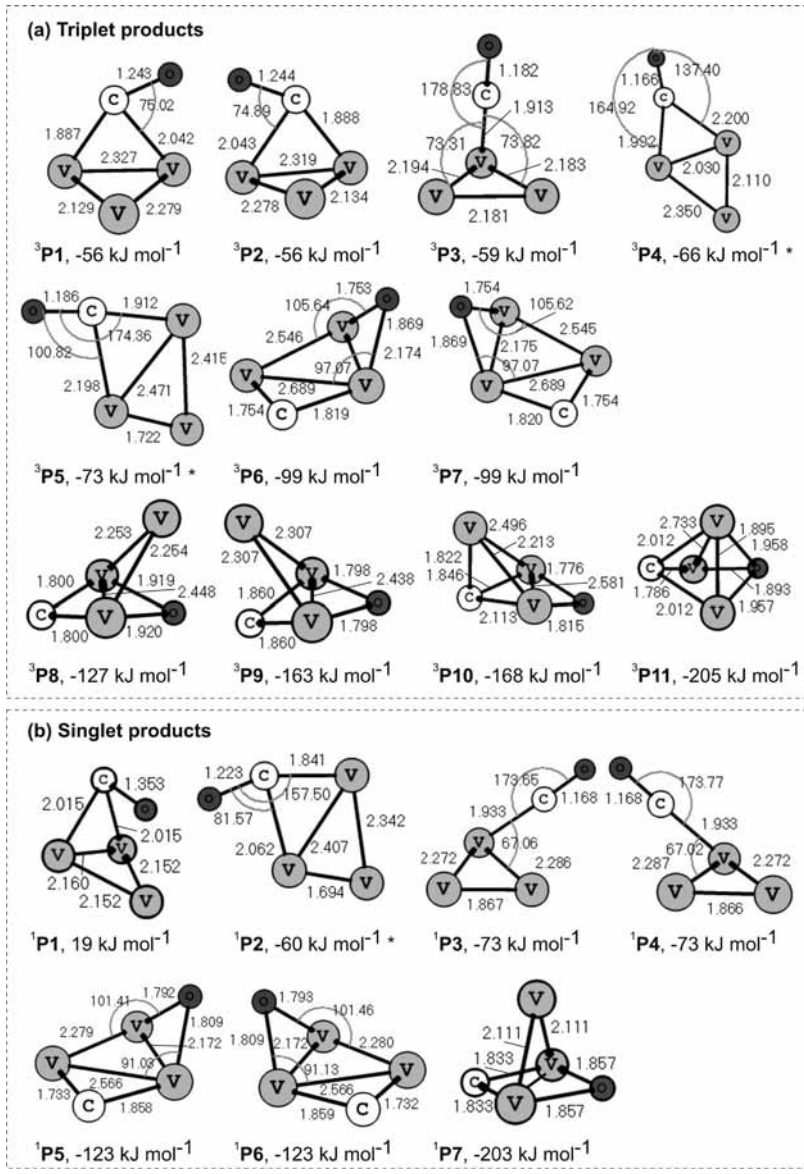

Figure 3. Optimized structures and relative energies of several $V_3(CO)^+$ and $V_3(O)(C)^+$ product ions on the (a) triplet and (b) singlet surface; energies are given relative to the entrance channel of the ground-state reactants. Bond angles and bond lengths (in Ångstroms) are given as well. Singlets and triplets are indicated by the superscripts 1 and 3, respectively. The structures ^{3}**P4**, ^{3}**P5**, ^{3}**P8**, ^{3}**P9**, ^{1}**P1**, ^{1}**P2**, and ^{1}**P7** are C_s-symmetric; all others have C_1 symmetry. *All of the atoms in the product structures ^{3}**P4**, ^{3}**P5**, and ^{1}**P2** are in a planar coordination.

dissociative binding of CO in the product ion. Figure 3 shows a range of conceivable products for the overall reaction of V_3^+ with methanol sorted by increasing thermodynamic stability. The observed product ions can be classified in three different groups, (a) vanadium clusters with an intact CO ligand bound in a mono- or bidentate fashion via the C- or O-atom to the cluster (^{3}**P1**−^{3}**P5**, ^{1}**P1**−^{1}**P4**), (b) product ions that contain a cleaved C−O bond with the (bridging) C- and O-atoms bound to different vanadium centers (^{3}**P6**−^{3}**P7**, ^{1}**P5**−^{1}**P6**), and (c) a cage-like structures with a cleaved C−O bond which binds the bridging C- and O-atom to identical vanadium atoms (^{3}**P8**−^{3}**P11**, ^{1}**P7**).

Quite clearly, while other structures than those shown in Figure 3 are conceivable, this set of structures chosen may suffice to establish a sensible correlation between the structure and thermochemical stability of the products formed.

On the triplet surface, the cationic product ions ^{3}**P1**, ^{3}**P2**, ^{3}**P3**, ^{3}**P4**, and ^{3}**P5** contain an intact CO unit that is bound via its C-atom to the V_3^+ cluster; energetically, they all fall in a comparable energy range of −56 to −73 kJ mol^{-1}. Interestingly, the monodentate carbonyl cluster that contains also an intact CO ligand bound to a single metal atom, like in ^{3}**P3**, is of similar stability as the bidentate carbonyl clusters (^{3}**P1**, ^{3}**P2**, ^{3}**P4**, and ^{3}**P5**). On the singlet surface, the energy range is more diverse for the $V_3(CO)^+$ cluster cations with an intact CO ligand. An endothermic product at 19 kJ mol^{-1} is obtained (Figure 3, ^{1}**P1**) as well as exothermic products ranging from −60 to −73 kJ mol^{-1} (Figure 3, ^{1}**P2**, ^{1}**P3**, ^{1}**P4**). Surprisingly, here, the monodentate carbonyl clusters (^{1}**P3** and ^{1}**P4**) are more stable than the bidentate species (^{1}**P1** and ^{1}**P2**). The above-discussed $V_3(CO)^+$ ions have in common a CO ligand attached to V_3^+ via the carbon atom. The bond lengths of the carbon monoxide ligands are all invariably elongated to various degrees as compared to free carbon monoxide (1.111 Å). This finding is indicative of π-backbonding causing a decrease of the bond order of the ligand. Product ions containing an intact CO ligand bound via the O-atom to the cluster, that is, $V_3(OC)^+$ instead of $V_3(CO)^+$, could not be located as minima for any V_3 cluster

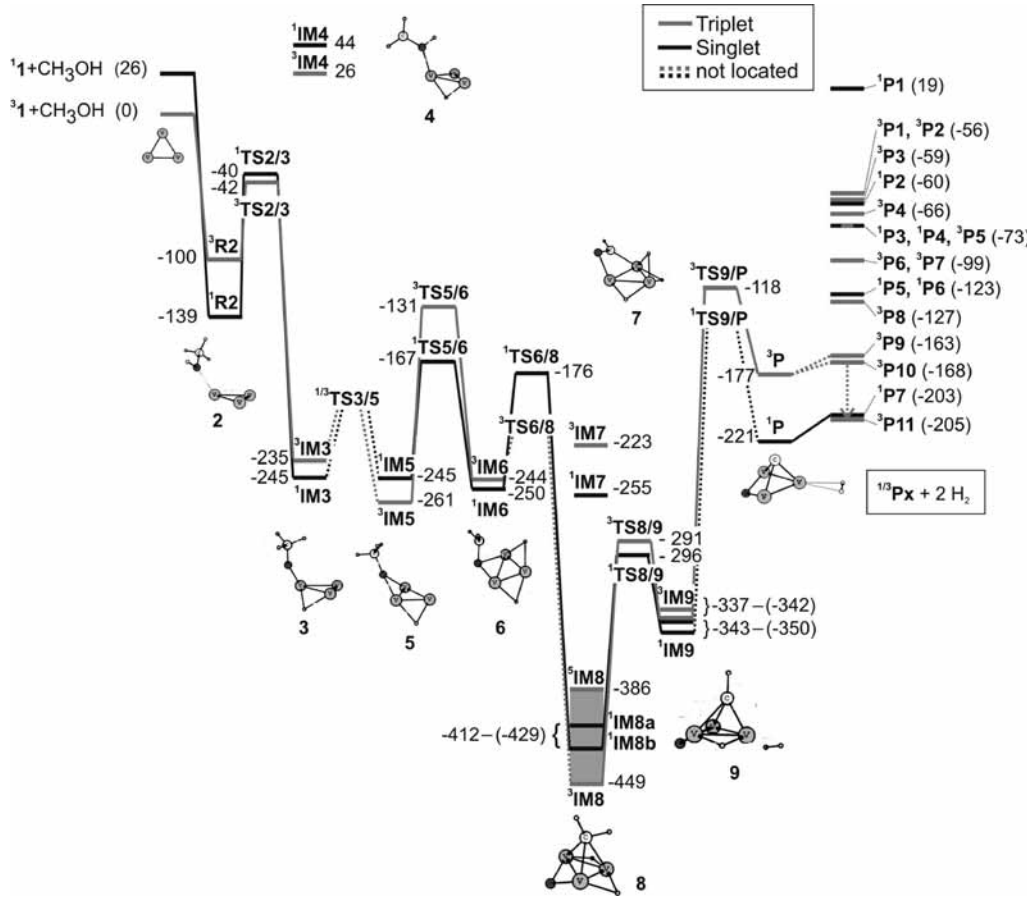

Figure 4. Relative energies of the reaction pathways for the complete dehydrogenation of methanol by V_3^+. The structures of reactants (R), transition structures (TS), intermediates (IM), and products (P) are given in Figuress 5 and 6. Singlet, triplet, and quintuplet states are indicated by the superscripts 1, 3, and 5, respectively.

structure considered. For the product ions with a cleaved C−O bond, much higher exothermicities of as much as −99 kJ mol^{-1} (Figure 3, ^{3}**P6** and ^{3}**P7**) on the triplet and at least −123 kJ mol^{-1} (Figure 3, ^{1}**P5** and ^{1}**P6**) on the singlet surface are predicted. All four structures consist of bridging C- and O-atoms to different vanadium sites of the cluster.

Finally, the cage-like structures which bind the bridging O- and C-atoms each to the same vanadium centers are thermochemically even more favored. Four product structures are located on the triplet surface (^{3}**P8**, ^{3}**P9**, ^{3}**P10**, and ^{3}**P11**). Obviously, the more compact the vanadium carbide structure in the cluster being formed, the more stable the product. An energetic minimum is obtained for the most densely "packed" cluster, ^{3}**P11**, at −205 kJ mol^{-1}, which we assign as the global minimum. The singlet surface to produce $V_3(O)(C)^+$ predicts also a cage-like C_s-symmetric product (^{1}**P7**: −203 kJ mol^{-1}, Figure 3) which is practically isoenergetic with the most stable product on the triplet surface.

The structures with a cleaved C−O bond formally correspond to an oxidative addition as the metal atoms with vacant coordination sites are oxidized by their insertion into the covalent C−O bond. The bond cleavage of the carbon monoxide ligand affords a bridging oxygen atom on one side of the metal cluster and a carbide on the other. The bond energy in CO that needs to be cleaved amounts to 1076 kJ mol^{-1}.[34] At first glance, this energy demand for C−O bond cleavage seems to constitute an insurmountably high obstacle. However, it can be compensated for by the formation of strong V−O and V−C bonds in the course of the reaction. Due to its thermochemical preference, in the following considerations about a conceivable reaction mechanism, we focus on the production of $V_3(O)(C)^+$ (i.e., ^{3}**P8**−^{3}**P11** and ^{1}**P5**−^{1}**P7**).

Reaction Mechanism. A possible reaction mechanism that accounts for the formation of the experimentally observed products starting from the ground-state reactants V_3^+/CH$_3$OH is briefly outlined in the following. Figure 4 illustrates the relative energies of the reaction pathway as proposed; here and in Figures 5 and 6, the computed geometries of the most relevant species are compiled.

The reaction of V_3^+ with methanol commences with the formation of the ion/molecule complex ^{3}**R2** (−100 kJ mol^{-1}) on the triplet and the more stable complex ^{1}**R2** (−139 kJ mol^{-1}) on the singlet surface. On both surfaces, the oxygen atom of methanol is attached to a single vanadium atom. As a consequence, the V_3^+ substructure deforms in that the neighboring V−V bonds elongate whereas the opposite V−V bond becomes shorter in comparison with the unperturbed V_3^+ cluster ion.

The next step corresponds to the transfer of the hydrogen atom from the hydroxy group to the cluster, yielding intermediates ^{3}**IM3** (−235 kJ mol^{-1}) and ^{1}**IM3** (−245 kJ mol^{-1}). The energy barrier for the initial hydrogen transfer lies for both multiplicities ∼40 kJ mol^{-1} below the entrance channel ($^{1/3}$**TS2/3**). In contrast, the energy barrier for the abstraction of a hydrogen atom from the methyl group in methanol cannot be surmounted. This hydrogen-transfer product is calculated to be endothermic by 26 kJ mol^{-1} (^{3}**IM4**) for the triplet and 44 kJ mol^{-1} (^{1}**IM4**) for the singlet species relative to the entrance channel, and this pathway is thus not pursued any further.

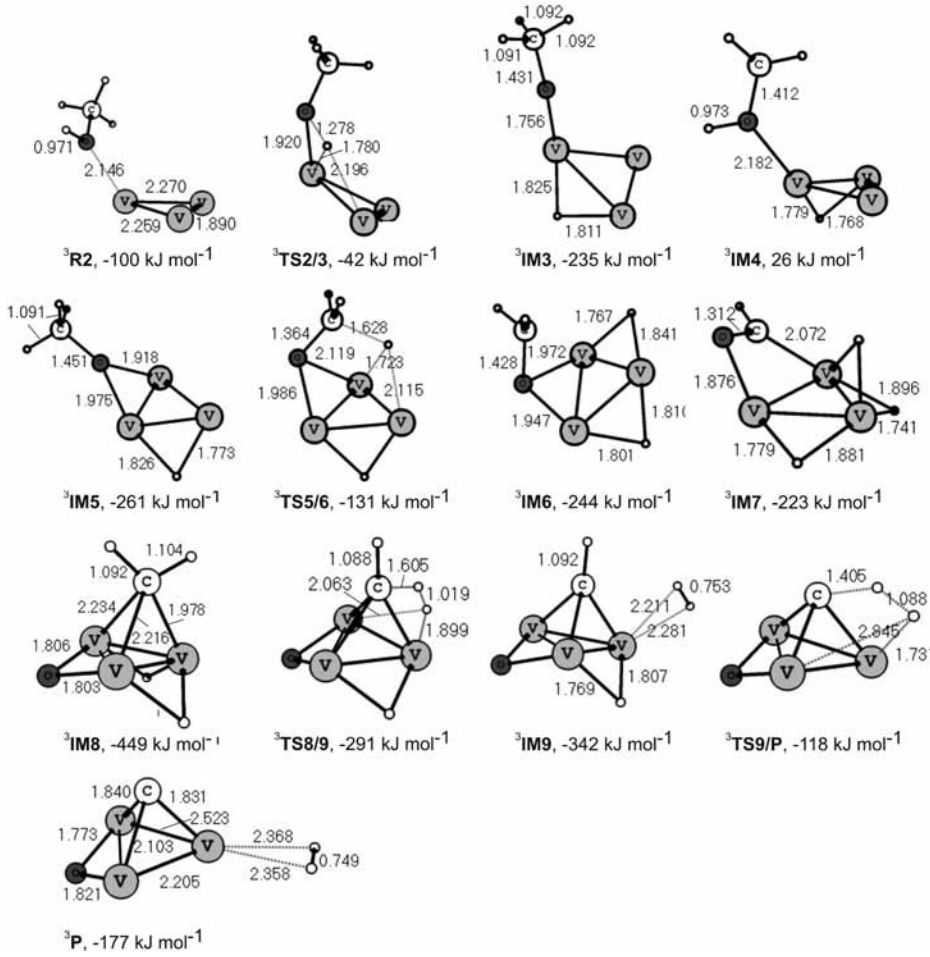

Figure 5. Reactant-like triplet intermediates and transition structures for the dehydrogenation of methanol by V_3^+. Bond lengths are given in Ångstroms, and triplets are indicated by the superscript 3.

Although only relatively minor energetic and structural differences occur, we were not able to locate the transition structures $^{1/3}$**TS3/5** to form the intermediates ^{3}**IM5** (−261 kJ mol^{-1}) and ^{1}**IM5** (−245 kJ mol^{-1}), respectively. However, the next hydrogen atom transfer stemming from the methyl group of the methoxy ligand to the vanadium cluster produces intermediates ^{3}**IM6** (−244 kJ mol^{-1}) and ^{1}**IM6** (−250 kJ mol^{-1}). The two latter structures contain a formaldehyde ligand and two hydrogen atoms bound to the vanadium cluster. Interestingly, the energy barrier of the singlet species (^{1}**TS5/6**) lies more than 50 kJ mol^{-1} below that of the triplet electromer (^{3}**TS5/6**).

The reaction may then proceed via transfer of a third hydrogen atom from the cluster to form ^{3}**IM7** (−223 kJ mol^{-1}) and ^{1}**IM7** (−255 kJ mol^{-1}). Nonetheless, the enormously exothermic step corresponding to an oxidative addition, initiated by the insertion of the vanadium cluster into the C−O bond entailing the latter's cleavage, is more likely to happen on energetic grounds. During the passage of ^{1}**TS6/8** on the singlet surface, the C−O bond stretches concomitant with positioning the methylene group between two vanadium atoms above the vanadium cluster and the bridging oxygen atom slightly underneath (Figure 6); an equivalent TS on the triplet surface could not be located. Eventually, the low-energy intermediates ^{3}**IM8** (−449 kJ mol^{-1})[35] and ^{1}**IM8a** (−412 kJ mol^{-1}) are formed. The process of C−O bond cleavage is accompanied by the formation of three new V−C bonds, which may serve as a reasonable explanation for the large energy gain of around 180 kJ mol^{-1}. On the singlet surface, the methylene group in ^{1}**IM8a** can undergo a rotation to produce slightly more stable ^{1}**IM8b** (−429 kJ mol^{-1}).

The next step corresponds to the migration of a hydrogen atom from the methylene group in order to release a hydrogen molecule from the cluster to produce $V_3OCH_2^+$ (^{1}**IM9** and ^{3}**IM9**). The corresponding energies for the ion/molecule complex $V_3OCH_2^+\cdots H_2$ as well as those for the separate cluster and hydrogen molecule $V_3OCH_2^+ + H_2$ amount to −342 and −337 kJ mol^{-1} (^{3}**IM9**) on the triplet and to −350 and −343 kJ mol^{-1} (^{1}**IM9**) on the singlet surface, respectively.

Further C−H bond cleavage may proceed via ^{3}**TS9/P** (−118 kJ mol^{-1}) associated with the transfer of the last hydrogen atom from the C−H group to the vanadium core to allow the generation of a second hydrogen molecule which still interacts with the product ^{3}**P** (−177 kJ mol^{-1}). While the associated transition structure could not be located on the singlet surface, the respective product ion interacting with H_2 (structure ^{1}**P**) is located at a relative energy of −221 kJ mol^{-1}. The release of a second H_2 molecule eventually affords the product ions ^{3}**P9** or ^{3}**P10** as triplet species and ^{1}**P7** on the singlet surface (Figure 4). On energetic grounds, in this reaction pathway, only postreactive rearrangements can form the compact cluster ^{3}**P11.**

In a more general sense, it is noteworthy that the minimum-energy pathway exhibits different multiplicities. For instance, the reaction starts on the triplet ground state; however, formation

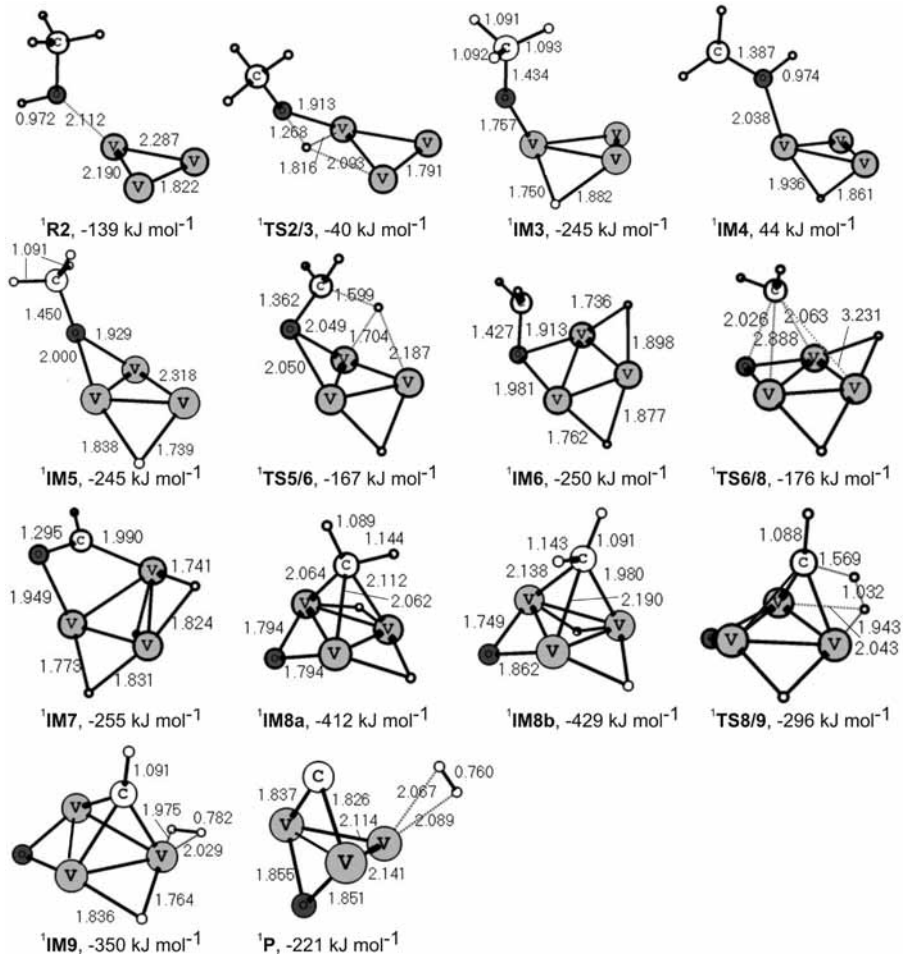

Figure 6. Reactant-like singlet intermediates and transition structures for the dehydrogenation of methanol by V_3^+. Bond lengths are given in Ångstroms, and singlets are indicated by the superscript 1. The structure ^{1}**IM8a** is C_s-symmetric.

of the encounter complex ^{1}**R2** is already energetically favored on the singlet surface, suggesting two-state reactivity (TSR) scenarios.[36]

Conclusion

The product distributions in the reactions of bare vanadium cluster cations with methanol are highly size-selective throughout the range of cluster sizes investigated. Each vanadium atom appears to count, meaning that by adding or removing a single atom, important changes in the reactivity properties of the molecular systems occur. While the atomic vanadium cation V^+ is rather reactive, it cannot mediate dehydrogenation of methanol but instead leads to the expulsion of methane and a methyl radical, respectively. Only clusters with three or more vanadium atoms efficiently bring about complete dehydrogenation of methanol to produce V_nOC^+ concomitant with the liberation of two H_2 molecules. The product ions as well as the potential energy surface of the V_3^+/methanol system have been investigated by means of extensive DFT calculations. The theoretical results strongly propose the occurrence of chemisorption to bring about the C−O bond cleavage ($\Delta_r H = -205$ kJ mol^{-1}) of the insipient CO ligand rather than its absorption as an intact molecule on the surface of the cluster ($\Delta_r H = -73$ kJ mol^{-1}). Further, the calculations indicate that the substantial reactivity difference between V_2^+ and V_3^+ in terms of dehydrogenation of methanol can be traced back to the minimal number of metal atoms in the cluster that are required to permit oxidative addition to take place. Apparently, two metal atoms are insufficient for inserting into the C−O bond to initiate its bond cleavage and to subsequently form the thermochemically favored ionic product with dissociative binding of the carbon monoxide molecule. On the other hand, the cationic trinuclear vanadium cluster seems to offer the minimal number of metal atoms to bring about oxidative addition; thus, the formation of three new V−C bonds overcomes the huge energy demand for C−O bond cleavage of 1076 kJ mol^{-1} (^{1}**TS6/8** in Figures 4 and 6).[34]

To conclude, bare vanadium cluster cations do not seem to serve as good models for catalytic purposes with respect to the recovering of the catalyst as the resulting carbon monoxide ligand upon dehydrogenation of the alcohol seems to be cleaved and irreversibly incorporated in the cluster. On the other hand, our studies suggest that for the reverse process, that is, hydrogenation of "CO", the minimal cluster size corresponds to $n \geq 3$.[37]

Acknowledgment. Financial support by the Deutsche Forschungsgemeinschaft (SFB 546), the Fonds der Chemischen Industrie, and the Czech Academy of Sciences (Z4055506) is gratefully acknowledged. We appreciate helpful comments by Prof. Dr. Joachim Sauer, Prof. Dr. Christoph van Wüllen, and Dr. Zoë Harvey with respect to the calculations. This work is dedicated to Professor Walter Thiel in recognition of his fundamental contributions to the understanding of catalysis on the occasion of his 60th birthday.

Supporting Information Available: The GGA optimized TZVP basis set for vanadium and the Cartesian coordinates of the computed structures. This material is available free of charge via the Internet at http://pubs.acs.org.

References and Notes

(1) Krenn, G.; Schennacha, K. *J. Chem. Phys.* **2004**, *120*, 5729.

(2) Shen, M.; Zaera, F. *J. Phys. Chem. C* **2008**, *112*, 1636.

(3) Ertl, G. *Surf. Sci.* **1993**, *287*, 1.

(4) King, D. A., Woodruff, D. W. Eds. *The Chemical Physics of Solid Surfaces and Heterogeneous Catalysis*; Elsevier: Amsterdam, The Netherlands, 1984; Vols. 2 and 3.

(5) Bell, A. T. *Science* **2003**, *299*, 1688.

(6) Jena, P.; Castleman, A. W., Jr. *Proc. Natl. Acad. Sci. U.S.A.* **2006**, *103*, 10560.

(7) (a) Armentrout, P. B. *Annu. Rev. Phys. Chem.* **2001**, *52*, 423. (b) Jackson, P.; Fisher, K. J.; Dance, I. G.; Gadd, G. E.; Willett, G. D. *J. Cluster Sci.* **2002**, *13*, 165. (c) Fisher, K. J. *Prog. Inorg. Chem.* **2001**, *50*, 343. (d) Armentrout, P. B. *Top. Curr. Chem.* **2003**, *225*, 233. (e) Böhme, D. K.; Schwarz, H. *Angew. Chem., Int. Ed.* **2005**, *44*, 2336. (f) O'Hair, R. A. J. *Chem. Commun.* **2006**, 1469.

(8) (a) Xu, J.; Rodgers, M. T.; Griffin, J. B.; Armentrout, P. B. *J. Chem. Phys.* **1998**, *108*, 9339. (b) Holmgren, L.; Rosen, A. *J. Chem. Phys.* **1998**, *110*, 2629. (c) Koszinowski, K.; Schröder, D.; Schwarz, H. *J. Phys. Chem. A* **2003**, *107*, 4999. (d) Burgert, R.; Schnöckel, H.; Grubisic, A.; Li, X.; Stokes, S. T.; Bowen, K. H.; Ganteför, G. F.; Kiran, B.; Jena, P. *Science* **2008**, *319*, 438.

(9) (a) Hagen, N. *Technische Katalyse, Eine Einführung*; Wiley-VCH: Weinheim, Germany, 1996. (b) Centi, G.; Cavani, F.; Trifirü, F. *Selective Oxidation by Heterogeneous Catalysis*; Plenum Publishers: New York, 2001.

(10) Nonose, S.; Sone, Y.; Kikuchi, Y.; Fuke, K.; Kaya, K. *Chem. Phys. Lett.* **1989**, *158*, 152.

(11) See also: (a) Dong, F.; Heinbuch, S.; Xie, Y.; Rocca, J. J.; Bernstein, E. R.; Wang, Z.-C.; Deng, K.; He, S.-G. *J. Am. Chem. Soc.* **2008**, *130*, 1932. (b) Dong, F.; Heinbuch, S.; Xie, Y.; Rocca, J. J.; Bernstein, E. R. *J. Phys. Chem. A* **2009**, *113*, 3029.

(12) For reactions of vanadium oxide cluster cations with methanol, see: (a) Justes, D. R.; Moore, N. A.; Castleman, A. W., Jr. *J. Phys. Chem. B* **2004**, *108*, 3855. (b) Feyel, S.; Scharfenberg, L.; Daniel, C.; Hartl, H.; Schröder, D.; Schwarz, H. *J. Phys. Chem. A* **2007**, *111*, 3278.

(13) For a characterization of related methoxo vanadium oxide cluster anions, see: Feyel, S.; Schwarz, H.; Schröder, D.; Daniel, C.; Hartl, Döbler, J.; Sauer, J.; Santambrogio, G.; Wöste, L.; Asmis, K. *ChemPhysChem* **2007**, *8*, 1640.

(14) (a) Eller, K.; Schwarz, H. *Int. J. Mass Spectrom. Ion Processes* **1989**, *93*, 243. (b) Engeser, M.; Schröder, D.; Weiske, T.; Schwarz, H. *J. Phys. Chem. A* **2003**, *107*, 2855.

(15) Forbes, R. A.; Laukien, F. H.; Wronka, J. *Int. J. Mass Spectrom. Ion Processes* **1988**, *83*, 23.

(16) In the generation of larger metal clusters with $n > 3$, the intensity decreases dramatically with cluster size. A doubling of the data accumulation only leads to an improvement of the signal-to-noise ratio of 10%, and thus, in this work bare metal cluster ions are only investigated quantitatively to $n = 5$ and qualitatively to $n = 7$.

(17) Bartmess, J. E.; Georgiadis, R. M. *Vacuum* **1983**, *33*, 149.

(18) Schröder, D.; Schwarz, H.; Clemmer, D. E.; Chen, Y.-M.; Armentrout, P. B.; Baranov, V. I.; Böhme, D. K. *Int. J. Mass Spectrom. Ion Processes* **1997**, *161*, 177.

(19) (a) Su, T. J. *J. Chem. Phys.* **1988**, *88*, 4102. (b) Su, T. J. *J. Chem. Phys.* **1988**, *89*, 5355.

(20) Frisch, M. J.; Trucks, G. W.; Schlegel, H. B.; Scuseria, G. E.; Robb, M. A.; Cheeseman, J. R.; Montgomery, J. A., Jr.; Vreven, T.; Kudin, K. N.; Burant, J. C.; Millam, J. M.; Iyengar, S. S.; Tomasi, J.; Barone, V.; Mennucci, B.; Cossi, M.; Scalmani, G.; Rega, N.; Petersson, G. A.; Nakatsuji, H.; Hada, M.; Ehara, M.; Toyota, K.; Fukuda, R.; Hasegawa, J.; Ishida, M.; Nakajima, T.; Honda, Y.; Kitao, O.; Nakai, H.; Klene, M.; Li, X.; Knox, J. E.; Hratchian, H. P.; Cross, J. B.; Bakken, V.; Adamo, C.; Jaramillo, J.; Gomperts, R.; Stratmann, R. E.; Yazyev, O.; Austin, A. J.; Cammi, R.; Pomelli, C.; Ochterski, J. W.; Ayala, P. Y.; Morokuma, K.; Voth, G. A.; Salvador, P.; Dannenberg, J. J.; Zakrzewski, V. G.; Dapprich, S.; Daniels, A. D.; Strain, M. C.; Farkas, O.; Malick, D. K.; Rabuck, A. D.; Raghavachari, K.; Foresman, J. B.; Ortiz, J. V.; Cui, Q.; Baboul, A. G.; Clifford, S.; Cioslowski, J.; Stefanov, B. B.; Liu, G.; Liashenko, A.; Piskorz, P.; Komaromi, I.; Martin, R. L.; Fox, D. J.; Keith, T.; Al-Laham, M. A.; Peng, C. Y.; Nanayakkara, A.; Challacombe, M.; Gill, P. M. W.; Johnson, B.; Chen, W.; Wong, M. W.; Gonzalez, C.; Pople, J. A. *Gaussian 03*, revision C.02; Gaussian, Inc.: Wallingford, CT, 2004.

(21) (a) Perdew, J. B.; Chevary, J. A.; Vosko, S. H.; Jackson, K. A.; Pederson, M. R.; Singh, D. J.; Fiolhais, C. *Phys. Rev. B* **1992**, *46*, 6671. (b) Perdew, J. B.; Burke, K.; Wang, Y. *Phys. Rev. B* **1996**, *54*, 16533.

(22) Vosko, S. H.; Wilk, L.; Nusair, M. *Can. J. Phys.* **1980**, *58*, 1200.

(23) Calaminici, P.; Köster, A. M.; Carrington, T., Jr.; Roy, P.-N.; Russo, N.; Salahub, D. R. *J. Chem. Phys.* **2001**, *114*, 4036.

(24) (a) Schäfer, A.; Huber, C.; Ahlrichs, R. *J. Chem. Phys.* **1994**, *100*, 5829. (b) Schäfer, A.; Horn, H.; Ahlrichs, R. *J. Chem. Phys.* **1992**, *97*, 2571.

(25) (a) Fukui, K. *J. Phys. Chem.* **1970**, *74*, 4161. (b) Fukui, K. *Acc. Chem. Res.* **1981**, *14*, 363. (c) Gonzalez, C.; Schlegel, H. B. *J. Phys. Chem.* **1990**, *94*, 5523.

(26) (a) Engeser, M.; Schröder, D.; Schwarz, H. *Chem.—Eur. J.* **2005**, *11*, 5975. (b) Schröder, D.; Engeser, M.; Schwarz, H.; Rosenthal, E. C. E.; Döbler, J.; Sauer, J. *Inorg. Chem.* **2006**, *45*, 6235.

(27) Bondybey, V. I.; Beyer, M. K. *J. Phys. Chem. A* **2001**, *105*, 951.

(28) Koyanagi, G. K.; Böhme, D. K.; Kretzschmar, I.; Schröder, D.; Schwarz, H. *J. Phys. Chem. A* **2001**, *105*, 4259.

(29) Blanksby, S. J.; Ellison, G. B. *Acc. Chem. Res.* **2003**, *36*, 255.

(30) Xu, J.; Rodgers, M. T.; Griffin, J. B.; Armentrout, P. B. *J. Chem. Phys.* **1998**, *108*, 9339.

(31) (a) Brönstrup, M.; Schröder, D.; Kretzschmar, I.; Schwarz, H.; Harvey, J. N. *J. Am. Chem. Soc.* **2001**, *123*, 142. (b) Koszinowski, K.; Schröder, D.; Schwarz, H. *Organometallics* **2004**, *23*, 1132. (c) Feyel, S.; Schröder, D.; Schwarz, H. *Eur. J. Inorg. Chem.* **2008**, *31*, 5961.

(32) Swart, I.; Fielicke, A.; Redlich, B.; Meijer, G.; Weckhuysen, B. M.; de Groot, F. M. F. *J. Am. Chem. Soc.* **2007**, *129*, 2516.

(33) (a) Pykavy, M.; van Wüllen, C. *J. Comput. Chem.* **2007**, *28*, 2252. (b) Rozanska, X.; Sauer, J. *Int. J. Quantum Chem.* **2008**, *108*, 2223. (c) Bande, A.; Lüchow, A. *Phys. Chem. Chem. Phys.* **2008**, *10*, 3371.

(34) Brewer, L.; Rosenblatt, G.; *Advances in High Temperature Science*; Academic Press: New York, 1969; Vol. 2.

(35) The results for the intermediate ^{3}**8** are affected by spin contamination, as indicated by a significant deviation of the expectation value of the total spin $\langle S^2 \rangle$ from a value of 2; that is, $\langle S^2 \rangle$ differs from $s(s + 1)$ by more than 10%. As spin contamination results in wave functions which appear to be the desired spin state but have some higher spin state mixed in, the energies of the quintet state are then taken as limiting estimates (^{5}**8**), as indicated by the grey-shaded box in Figure 4. For further comments, see: http://www.ccl.net/cca/documents/dyoung/topics-orig/spin-cont.html.

(36) (a) Schröder, D.; Shaik, S.; Schwarz, H. *Acc. Chem. Res.* **2000**, *33*, 139. (b) Schwarz, H. *Int. J. Mass Spectrom.* **2004**, *237*, 75. (c) Carpenter, B. K. *Chem. Soc. Rev.* **2006**, *35*, 736. (d) Harvey, J. N. *Phys. Chem. Chem. Phys.* **2007**, *9*, 331. (e) Shaik, S.; Hirao, H.; Kumar, D. *Acc. Chem. Res.* **2007**, *40*, 532.

(37) For the dehydrogenative decarbonylation of a methoxy group by bare Fe^+, that is, the gas-phase reversal of Fischer/Tropsch synthesis, see: Prüsse, T.; Fiedler, A.; Schwarz, H. *J. Am. Chem. Soc.* **1991**, *113*, 8335.

JP901565R